Magnetic properties of arrays of superconducting strips in a perpendicular field

Enric Pardo,[1] Alvaro Sanchez,[1] and Carles Navau[1,2]

[1]*Grup d'Electromagnetisme, Departament de Física, Universitat Autònoma Barcelona, 08193 Bellaterra (Barcelona), Catalonia, Spain*
[2]*Escola Universitària Salesiana de Sarrià, Passeig Sant Joan Bosco 74, 08017 Barcelona, Catalonia, Spain*

Current profiles and field lines and magnetization and ac losses are calculated for arrays of infinitely long superconducting strips in the critical state in a perpendicularly applied magnetic field. The strips are arranged vertically, horizontally, and in a matrix configuration, which are the geometries found in many actual high-T_c superconducting tapes. The finite thickness of the strips and the effects of demagnetizing fields are considered. Systematic results for the magnetization and ac losses of the arrays are obtained as function of the geometry and separation of the constituent strips. Results allow us to understand some unexplained features observed in experiments, as well as to propose some future directions.

I. INTRODUCTION

High-temperature superconducting (HTSC) cables have a large potential for many applications where very high current intensities are needed, such as power transmission cables, magnets, superconducting magnetic energy storage systems, transformers, and motors.[1,2] In particular, silver-sheathed $Bi_2Sr_2Ca_2Cu_3O_{10}$ (Ag/Bi-2223) tape conductors appeared to be the HTSC most used for practical devices, due to the good superconductor material quality and the feasibility to make kilometer-long cables. Many of the HTSC cables applications work under ac conditions, like power transmission cables, transformers, and motors. An important problem for the superconducting power devices operating at ac intensities is caused by their power losses,[3] which must be reduced as low as possible to justify the expenses of the superconducting material and the cryogenic system. We can distinguish between self-field ac losses, that is, the power losses due to transport current inside each conductor, and the magnetic ac losses due to a magnetic field external to the conductor, which we deal with in this work. The latter kind of losses are important for devices where a high magnetic field is present, like magnets and transformers.

Magnetic ac losses critically depend on the superconductor wire geometry.[4,5] As was pointed out in Refs. 4–6, dividing the superconductor wire into filaments reduces the magnetic losses. Moreover, it is known that dividing superconducting wires into filaments and immersing them into a conducting matrix makes the wire more reliable under quenching.[4,5] In addition, it is shown that for Ag/Bi-2223 tapes, the superconducting properties improve when the superconducting region is divided into filaments with a high aspect ratio.[7,8] For these reasons, the latter is the HTSC wire geometry most often met in practice.

The magnetic ac losses in multifilamentary tapes have their origin in mainly three mechanisms. They are the eddy currents in the conducting sheath, the magnetic hysteresis arising from the flux pinning in the superconductor, and the interfilament currents (also known as coupling currents) that flow across the conducting matrix.[4,5] Although it is somehow understood how to reduce the eddy and coupling currents losses,[9,10] important work remains to be done concerning the

hysteresis losses. Many experimental works showed that the hysteresis losses depend strongly on the orientation of the external ac field.[11–13] It is shown that the hysteresis losses under an applied field H_a perpendicular to the wide face of the HTSC tapes are more than one order of magnitude higher than if H_a is either parallel to the wide face or in the transport direction.

A very convenient way to study hysteresis in superconductors is within the framework of the critical-state model,[14] which assumes that currents circulating in the SC's flow with a constant density J_c, later extended to currents depending only upon the local magnetic field H_i.[15] The original model was solved in the parallel geometry, that is, for applied fields H_a along an infinite dimension for slabs and cylinders,[14–16] because in these geometries the problem of the demagnetizing effects was not present. A further step was presented when the critical-state model was extended to the case of very thin strips[18–20] and disks,[21–23] for which important demagnetizing fields were involved. More recently, the more general case of a critical state in samples with finite thickness, such as strips[24] and cylinders,[25–27] was solved by numerical models.

In spite of this progress, there is no theoretical model that satisfactorily describes the losses of multifilamentary tapes under perpendicular H_a.[28,29] This general problem has not been systematically solved, although there have been some works offering partial solutions. Fabbricatore *et al.*[30] presented a comprehensive analysis of the Meissner state in arrays of strip lines arranged vertically (z stack of strips), horizontally (x arrays) and in the form of a matrix (xz array) and compared their results with actual measurements on multifilamentary tapes. Their numerical procedure, however, was not adequate to study the more general case of bulk current penetration. Mawatari[31] studied not only the Meissner state but also the critical state for the case of an infinite set of superconducting strip lines arranged periodically in the vertical or horizontal directions, in the limit that the strip lines were infinitely thin. Mawatari and Clem[32] studied the penetration of magnetic flux into current-carrying (infinitely thin) strips lines with slits in the absence of applied magnetic field. All the existing models assume either arrays of infinitely thin strips in the critical state or arrays of strips with

finite thickness but only in the Meissner state. The only exception we know is the recent work by Tebano *et al.*[33] in which preliminary results on the current penetration and magnetization were calculated for some realistic arrays based on the procedure developed by Brandt.[24]

A key issue in the study of superconducting tapes is how currents circulate in the filaments. There are two important cases concerning this point, depending on whether the current in each filament is restricted to go and return through the same filament or if there is no such restriction. The desired case for ac magnetic losses reduction in real HTSC tapes occurs when current is restricted to return through the same filament.[4-6,34] We refer to this case as isolated filaments. The other case is when current can go in one direction in a given filament and return through any other one. We refer to the latter case as completely interconnected filaments. This is the limiting case of filaments with a high number of intergrowths[35-39] or when coupling currents through the conducting matrix are of the same magnitude as the superconducting currents.[10,34,40,41] As explained in these references and below, the magnetic behavior for each of these two filament connection case is strongly different. Therefore, a detailed study of ac losses in superconducting cables should include these two cases. The strong difference in considering interconnected or isolated strips can be realized in the current profiles field lines shown in Figs. 6 and 7 for matrix arrays.

In this paper we study the current and field penetrations, magnetization, and ac losses of arrays of superconducting strips of finite thickness. We first present the model and its application to the case of an array of a finite number of infinitely long strips of finite thickness arranged vertically (z stack of finite strips) with a perpendicular applied field. This geometry is studied first because it is independent of the connection type, since as a result of the system symmetry, current always go and return through each strip. We then study the cases of horizontal (x) arrays and matrices (xz matrix), for which different behaviors arise depending on the connections. In all cases, we will concentrate our study on arrays composed of strips with high aspect ratio since this is the case most often met with in practice, although our model is applicable to arrays of strips with arbitrary thickness. Our approach, therefore, is more general than assuming the approximation of considering infinitely thin strips as in Ref. 31, since we take into account the different current penetration across the superconductor thickness.

The paper is structured as follows. In Sec. II we present the calculation model. Current and field profiles are calculated and discussed in Sec. III. The results of magnetization and magnetic ac losses are discussed in Sec. IV and V, respectively. Finally, in Sec. VI we present the main conclusions of this work. The full penetration fields for x arrays and xz matrices can be analytically calculated, being described in Appendix A, whereas the analytical formulas for the inductances used in the model are described in Appendix B.

II. MODEL

A. General formulation and vertical array case

The model we present here is suitable for any superconductor geometry with translational symmetry along the y axis

and mirror symmetry to the vertical plane. However, we will focus on z stacks, x arrays, and xz matrices made up of identical strips infinitely long in the y direction.

Our numerical model is based on minimizing the magnetic energy of the current distribution after each applied field variation. We name this model the minimum magnetic energy variation procedure, thereafter referred to as MMEV. The model assumes that there is no equilibrium magnetization in the superconductor. In this paper, we further assume that there is no field dependence of J_c for simplicity. The energy and flux minimization in the critical state was previously discussed by Badia *et al.*[42] and Chaddah and co-workers.[43,44] The details of the general numerical model can be found in Refs. 27 and 45–47. The approach has been successfully applied to describe the experimental features observed in the initial magnetization slope[45] as well as the whole magnetization loop and levitation force[27,46] of superconducting cylinders. We now outline the main characteristics of the model.

For cylindrical geometry,[45,27,46] the superconducting region was divided into a certain number of elements of the shape of rings with rectangular cross section, which formed circular closed circuits. For a given current distribution in the cylinder, the energy variation of setting a new current in a certain element was calculated. The minimum energy variation method consists in, given an applied field H_a, looking for the circuit which lowers the most the magnetic energy and set there a new current of magnitude J_c, and then repeating the procedure until setting any new current does not reduce the energy. The method as explained above is used to find the initial magnetization curve $M_i(H_a)$. Provided that J_c is field independent, the reverse curve can be found using that[23]

$$M_{\text{rev}}(H_a) = M_i(H_m) - 2M_i[(H_m - H_a)/2] \qquad (1)$$

and the returning curve using

$$M_{\text{ret}}(H_a) = -M_{\text{rev}}(-H_a), \qquad (2)$$

where H_m is the maximum applied field in the loop.

In the present case of arrays of superconducting strips, we divide each strip into a set of $2n_x \times 2n_z$ elements with cross section $(\Delta x)(\Delta z)$ and an infinite length in y direction, as shown in Fig. 1. The horizontal and vertical dimensions of the strips are $2a$ and $2b$, respectively. The dimensions of each element are $\Delta x = a/n_x$ and $\Delta y = b/n_z$. The separation of the xz-matrix rows is h and the separation of columns is d. A z stack and an x array can be considered as a matrix with a single column and row, respectively, as shown in Fig. 1. We consider that the current density is uniform within the elements and flows through the whole element section and not only through a linear circuit as in Refs. 27, 45, and 46. A spatially uniform applied field H_a in the z direction is considered.

The main condition for applying the model is that one has to know in advance the direction of currents. In the case of x arrays and xz-matrix arrays this issue has to be dealt with carefully; we will discuss about it in the next section. However, the case of a z stack presents no difficulty since in this
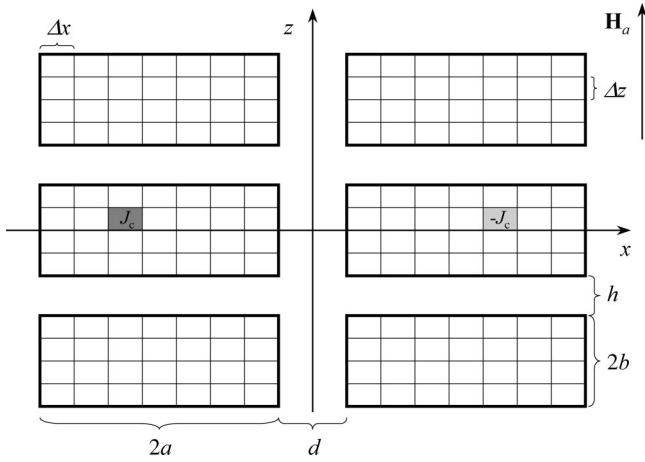
FIG. 1. Sketch of the array of superconducting strips. An xz matrix is drawn, although all the parameters described are also valid for z stacks (corresponding to a single column of strips) and x arrays (corresponding to a single row of strips). The y axis is perpendicular to the plane and it is oriented inwards.

case the induced current front is also symmetrical with respect to the zy plane. Thus, we can consider that the pair of elements centered at (x,z) and $(-x,z)$ form circuits that are closed at infinity. This grouping in pairs, forming closed circuits, allows for the analytical calculation of self- and mutual inductances per unit length of the circuits with finite cross section (see Appendix B for inductance derivations and formulas). The pairs, or circuits, are labeled using the subscript i from 1 to $N=2n_x n_z n_f$, n_f being the number of strips of the set and N the total number of elements in the $x \geqslant 0$ portion of the set of strips.

Once the analytical expressions for the inductances are obtained, the energy of the i circuit can be calculated as

$$E_i = \sum_{\substack{j=1 \\ j \neq i}}^{N} M_{ij} I_j I_i + \frac{1}{2} M_{ii} I_i^2 + 2\mu_0 H_a x_i I_i, \qquad (3)$$

where the first two terms are the energy of the circuit owing to the presence of the current distribution in the whole superconducting region, the third term is the energy due to the uniform applied magnetic field, M_{ij} are the self- and mutual inductances from Eqs. (B5)–(B7), and I_i and I_j are the total current intensity that flows through the circuits labeled as i and j, respectively. Since no internal field dependence is considered for the critical current, $|I_i| = (\Delta x)(\Delta z)J_c$. The sign of I_i is taken as positive when the current of the element at $x \geqslant 0$ of the pair follows the positive y axis direction and negative otherwise.

In the initial magnetization curve, after using the energy minimization procedure for a given applied field H_a to find the current profile, we can calculate the magnetization, the total magnetic field, and the magnetic field lines directly from the current distribution.

The magnetization, defined as the magnetic moment per unit volume, has only one nonzero component M_z, which can be calculated as

$$M_z = \frac{m_z}{4abn_f} = \frac{1}{4abn_f} \sum_{i=1}^{N} I_i(2x_i), \qquad (4)$$

where m_z is the total magnetic moment of the set of strips.

The two nonzero components of the total magnetic flux density, B_z and B_x, are calculated as the addition of all the closed-circuit contributions, which can be calculated analytically integrating the Biot-Savart law.[48]

The magnetic flux lines are calculated as in Ref. 24 using that for translational symmetry the level curves of the y component of the vector potential, for the gauge $\nabla \cdot \mathbf{A} = 0$, can be taken as the magnetic flux lines. The y component of the vector potential results from the contribution of all the elements pairs $A_{y,i}$, whose analytical expressions are Eqs. (B2)–(B4).

We will consider the application of an external ac field $H_a = H_m \cos(\omega t)$. In this case we can calculate the imaginary part of the ac susceptibility, χ'', defined as

$$\chi'' = \frac{2}{\pi H_m} \int_0^{\pi} d\theta M_{\text{rev}}(\theta) \sin\theta = \frac{2}{\pi H_m^2} \int_{-H_m}^{H_m} dH_a M_{\text{rev}}(H_a). \tag{5}$$

The energy loss W per ac cycle of amplitude H_a is related to χ'' by the expression[59,23]

$$W = \mu_0 \pi H_m^2 \chi''. \tag{6}$$

B. Horizontal and matrix array cases

As explained above, for the cases of x arrays and xz matrices we need to consider two different cases of filament connection—when the filaments are all interconnected or when they are isolated to each other—so the model presented above has to be generalized to include these cases.

We now discuss two features that are needed to apply the MMEV procedure to any superconductor geometry; this will help us to determine which modifications, if necessary, have to be done to adapt the MMEV procedure to x arrays and xz matrices.

The first condition to apply the MMEV procedure is that one needs to know the shape of the closed current loops of the magnetically induced current for any applied field value H_a. For cylinders the closed current loops were simply circular,[27,46] while for z stacks they are made up by an infinite straight current in the y direction centered at (x,z) and by another centered at $(-x,z)$, which form a closed circuit at infinity.

Another feature that has to be taken into account in order to apply the numerical method described in this work to x arrays and xz matrices is the sign of the induced current, once the shape of the closed current loops is known. For geometries such as rectangular strips and disks,[17,24,49,23] elliptical tapes,[49–51] and z stacks,[31] current in the initial magnetization curve is the same for all circuits. However, this feature it is not so obvious for geometries with gaps in the horizontal direction like x arrays and xz matrices.

As explained in the following subsections, the applicability of the two features mentioned is different when consider-

ing interconnected or isolated strips. So the adaptation of the MMEV procedure to the two different connection cases must be considered separately.

1. Interconnected strips

For the present case of x arrays and xz matrices with completely interconnected strips the two features presented above are the same as the cases of cylinders and z stacks presented above. This can be justified as follows.

First, the closed circuits to be used in the simulations are the same as for z stacks, which are each pair of current elements centered at (x,z) and $(-x,z)$, Fig. 1. This is due to the mirror yz symmetry of the system and the fact that the strips are interconnected at infinity so that currents belonging to different strips can be closed.

Second, the fact that in the initial magnetization curve the current is negative in all the circuits is also valid for the present case. We arrived at this conclusion after doing some preliminary numerical calculations, in which we changed the original numerical method, letting the procedure to choose which sign in each circuit is optimum to minimize the energy. After doing so, we saw that in the initial magnetization curve and for a given H_a, current is the same and negative for all circuits, except for very few circuits on the final current profile due to numerical error. Notice that this means that the current of the strips at the $x \geqslant 0$ region return to those in the $x \leqslant 0$ region, so that current return through different strips for all circuits except for those centered at $x=0$. This result is the expected one, because this situation is the one that minimizes the most the energy, so it should be the chosen one when there are no restrictions.

Then, we conclude that the numerical method and formulas for x arrays and xz matrices are the same as those previously used for z stacks with the only modifications needed for adapting the model to the new geometry.

2. Isolated strips

The model used to describe current isolated strips must take into account that all real current loops have to be closed inside each strip, so that there has to be the same amount of current following the negative y direction than the positive one inside each strip. In addition, although the current distribution of the whole x array or xz matrix has yz mirror symmetry for the plane $x=0$, the current distribution in the individual strips is not necessarily symmetrical to their vertical central plane.

Then, the features of the MMEV procedure described above do not apply, so that we need to do significant modifications to the original numerical procedure presented above.

The actual current loops in this case have the shape of two straight lines within the same strip carrying opposite currents and closed at infinity (solid lines in Fig. 2). These straight currents can be identified with the elements which the strips are divided in. The main difficulty is to know which pairs of elements describe closed current loops.

To help solving this problem we notice that, thanks to the overall mirror symmetry to the yz plane at $x=0$, for any
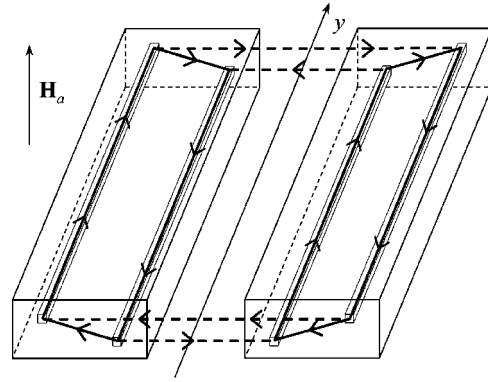

FIG. 2. Sketch of the real closed current loops (solid thick lines) and those used in the simulation (dashed thick lines). The case of an x array with two strips is drawn for simplicity. Four current elements are represented as elongated thin rectangular prisms where a single straight current flows following the y axis.

closed current loop in a strip at the $x \geqslant 0$ zone, there is another current loop set symmetrically in the corresponding strip in the $x \leqslant 0$ zone (Fig. 2). Furthermore, if we take as closed current loops the pairs of elements set symmetrically to the yz plane (dashed lines in Fig. 2), the total current distribution is the same except at the ends, which do not modify the magnetic moment if we consider the strips long enough. Both systems of closed circuits have the same magnetic properties, including magnetic energy and magnetic moment. Consequently, since these symmetrical pairs of elements correspond to the closed loops used for z stacks, all the formulas presented for that case are still applicable.

Taking these symmetrical pairs of elements as closed loops for the numerical procedure, as done in Sec. II B 1 for interconnected strips and the fact that current loops must close inside each strip, the MMEV procedure for isolated strips becomes the following in this case.

(1) For a given applied field H_a, a given current distribution, and for each pair of strips set symmetrically to the yz plane (symmetrical pair of strips), there are found: (i) the loop where setting a negative current would reduce the most the magnetic energy and ii) the loop where setting a positive current would rise it the least. These loops are referred to as a pair of loops.

(2) The pair of loops that lower the most the magnetic energy is selected among all those belonging to each symmetrical pair of strips.

(3) A current of the corresponding sign is set in the selected loops.

(4) This procedure is repeated until setting current in the most energy-reducing pair of loops would not decrease the magnetic energy.

Notice that each pair of loops where current is set in the simulations describes two real closed current loops belonging to each strip that constitute the symmetrical pair of strips.

III. CURRENT PENETRATION AND FIELD LINES

A. Vertical stacks

The most important issue to study in the system of superconducting strips is the influence of magnetic coupling. It is
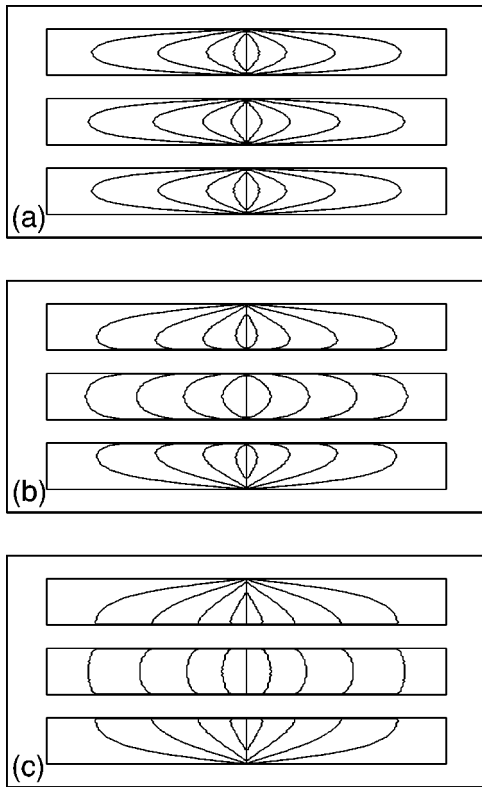
FIG. 3. Current profiles for a z stack of three superconducting strips of width $2a$ and height $2b$ separated a distance (a) $h/a = 2$, (b) $h/a = 0.2$, and (c) $h/a = 0.02$. The profiles correspond to applied fields $H_a/H_{pen} = 0.2$, 0.4, 0.6, 0.8, and 1, where H_{pen} is the penetration field of the array. For the sake of clarity, the separation, thickness, and width of strips are not on scale.

FIG. 4. Field lines corresponding to an applied field $H_a/H_{pen} = 0.4$, where H_{pen} is the penetration field of the z stack, for the stacks of Fig. 3. Right and left figures correspond to the total and self-field magnetic field lines, respectively. The distances are $d/a = 2$ (a),(b), 0.2 (c),(d), and 0.02 (e),(f).

well known that the superconductors tend to shield the magnetic field change not only in their interior but also in the space between two superconducting regions (as illustrated in the classical example of a hollow superconducting tube, for which the whole volume inside the tube and not only the tube walls are shielded). In our array of superconducting strips one should observe a related effect, because the current induced in the strips will tend to shield the magnetic field in their interior as well in the space between them. To study this effect we present in Fig. 3 calculations corresponding to a vertical array of three strips with $b/a = 0.1$ and different separations ($h = 2a$, $h = 0.2a$, and $h = 0.02a$, respectively). The different profiles correspond to applied fields $H_a/H_{pen} = 0.2$, 0.4, 0.6, 0.8, and 1, where H_{pen} is the field at which the array is fully penetrated by current (the calculation of such a field is discussed in Appendix A). The results show unambiguously the strong influence of magnetic coupling in the case that the separation is small, as illustrated in the case for $h = 0.02a$, for which the current profiles are almost the same as if there were no gaps between the strips. On the other hand, the case $h = 2a$ is already an example of a very weak magnetic coupling, which results in a current penetration for each strip almost as if the two others were not present.

To further study this point we present in Fig. 4 the field lines calculated for the three arrays of Fig. 3, for applied
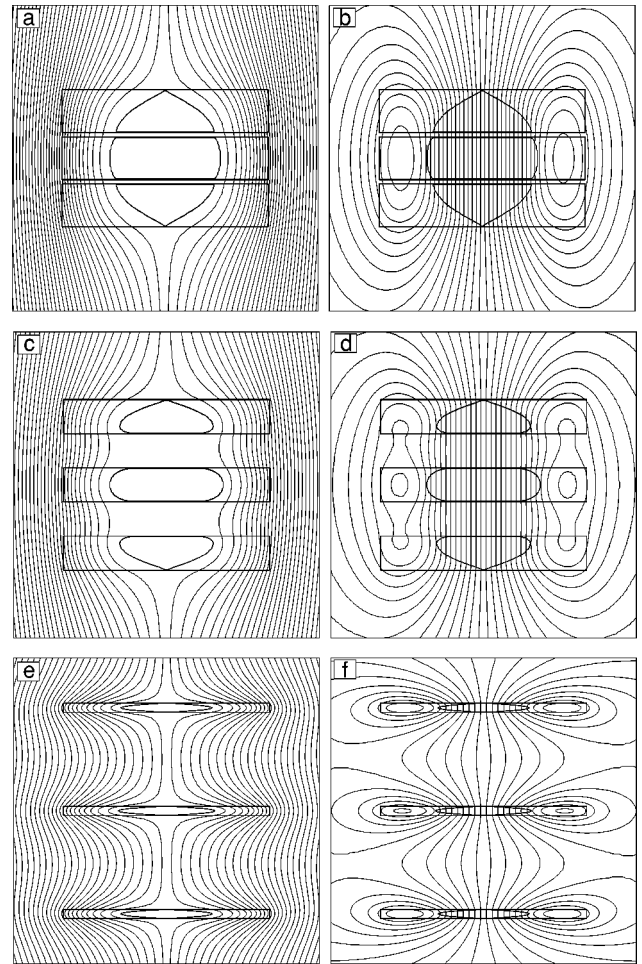
fields $H_a/H_{pen} = 0.4$. The left images show the total field and the right ones only the field created by the currents in the superconductor. It is clear that for $h = 0.02a$ and even $h = 0.2a$, the applied field in the space between superconductors is basically shielded by them, in contrast with the case of $h = 2a$, for which the magnetic field is modified near each strip but not enough to make a significant contribution to the other two strips. Another way of seeing this effect is illustrated in the calculations of the field created by currents (right images in each figure). One can observe that in all cases currents create a basically constant field in the spaces between strips. However, when the separation is large the total field lines created by the current are wrapped around each strip, whereas when the separation decreases up to $h/a = 0.02$ the field lines are hardly distinguishable from the case of the three strips forming a single thicker one.

B. Horizontal and matrix arrays

For the sake of clarity, we discuss separately the results corresponding to the situation in which strips are interconnected and that in which they are isolated.
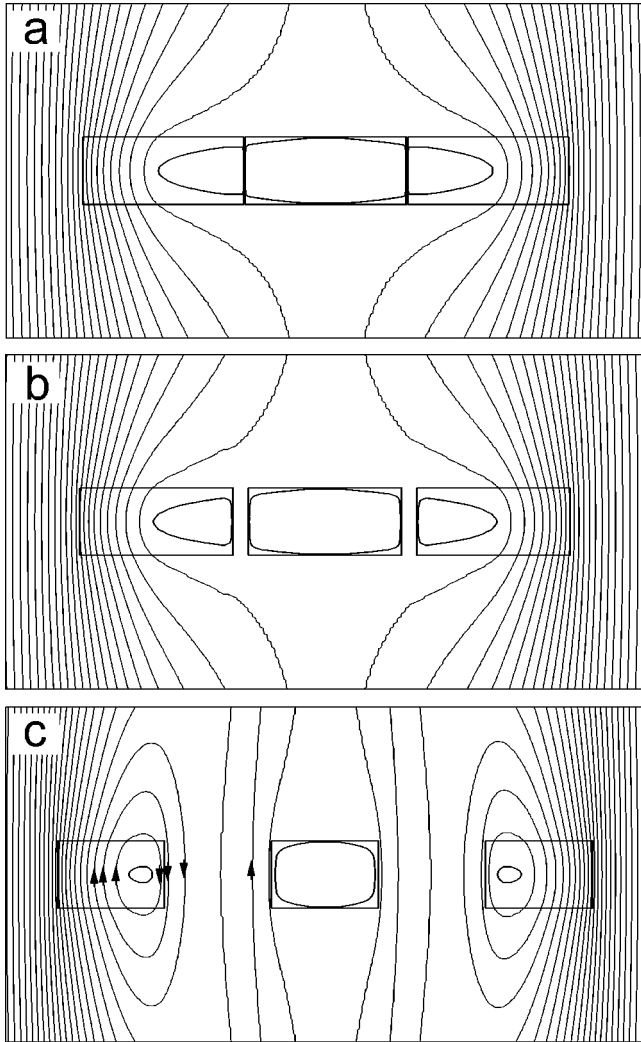
FIG. 5. Total magnetic field lines and current profiles for interconnected x arrays at an applied field of $H_a = 0.2H_{pen}$, H_{pen} being the complete penetration field for the whole x array. The strips in the arrays have an aspect ratio $b/a = 0.1$ and the distances between strips are (a) $d/a = 0.02$, (b) $d/a = 0.2$, and (c) $d/a = 2$. The horizontal scale has been contracted for clarity, while the vertical scale is the same for all figures.

1. Interconnected strips

We first discuss the current profiles and field lines calculated for an x array composed of three filaments with dimensions $b/a = 0.1$. In Fig. 5 we show the current profiles and the field lines corresponding to three x arrays with varying separation between the individual strips. The applied field in all cases is $0.2H_{pen}$, H_{pen} being the penetration field for the whole x array (Appendix A). The common behavior observed is that currents are induced to try to shield not only the superconductors (the field is zero in the current-free regions inside the superconductors) but also the space between them. Actually, we find that there appears an overshielding near the inner edge of the external strips (Fig. 5), so that the field there is opposite to the external field. This feature has been previously predicted for rings in the critical state[52] and for completely shielded toroids.[53]
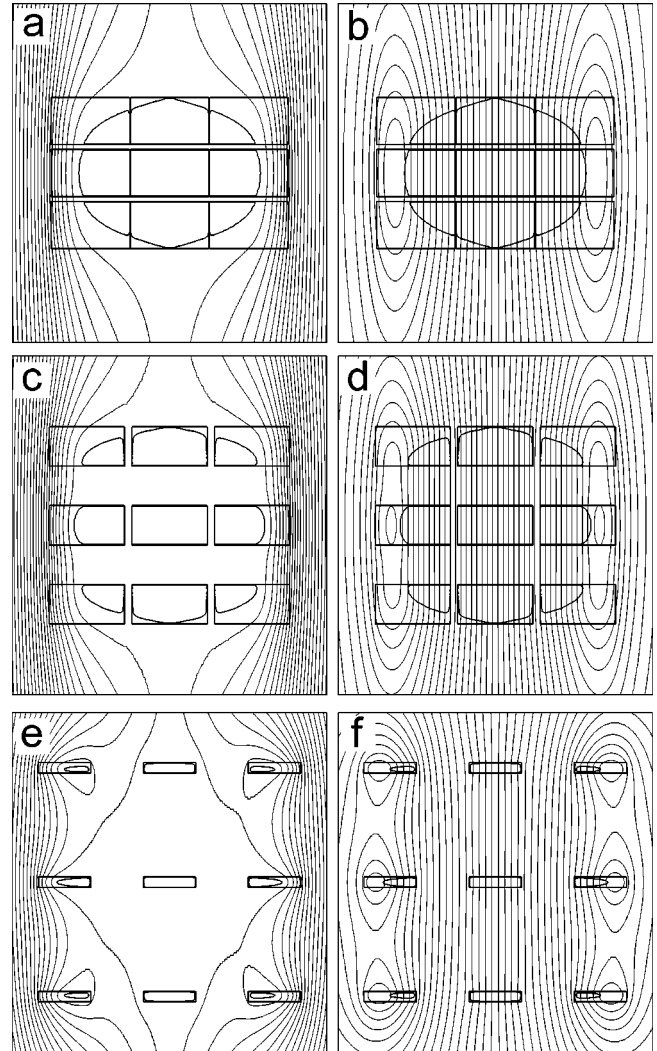

FIG. 6. Total (left) and self (right) magnetic field lines and current profiles for interconnected xz matrices at an applied field of $H_a = 0.2H_{pen}$. For the strips $b/a = 0.1$ and $d/a = h/a = 0.02$ (a),(b), 0.2 (c),(d), and 2 (e),(f). Vertical and horizontal scales are rescaled for clarity.

The general trends described above for the case of an x array are also valid for the case of an xz matrix. Actually, it is important to remark that the general trends in current and field penetration and the magnetic behavior of an xz matrix result from the composition of the properties of both the x array and the z stack that forms it. In Fig. 6 we show the calculated current penetration profiles for an xz matrix made of nine strips (3×3), each with dimensions $b/a = 0.1$ corresponding to an applied field of $0.2H_{pen}$. We also plot the total (left figures) and self (right figures) magnetic field, that is, the sum of the external magnetic field plus that created by the superconducting currents and only the latter contribution, respectively. The general trend of shielding the internal volume of the region bounded by the superconductor, including gaps between strips, is also clearly seen. An interesting feature is that a very satisfactory magnetic shielding is achieved for the three different matrices, as illustrated from the fact that the self-field in the central region has in all cases a constant
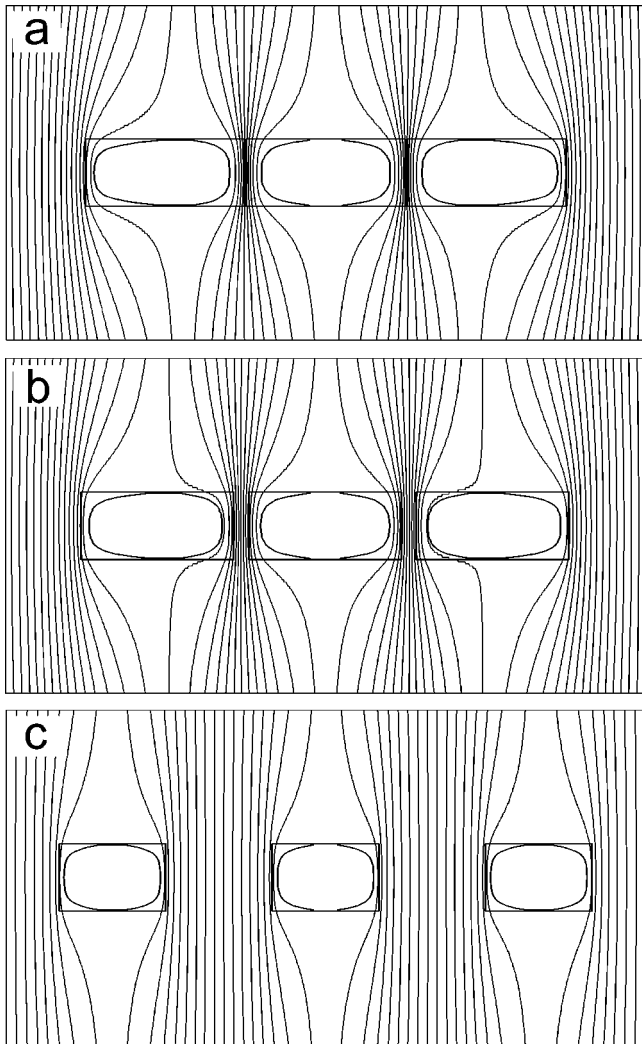
FIG. 7. The same as Fig. 5 but with isolated strips. The applied field is $H_a = 0.1 H_{pen}$ and the strips have dimensions $b/a = 0.1$ spaced a distance (a) $d/a = 0.02$, (b) $d/a = 0.2$, and (c) $d/a = 2$. The horizontal scale has been contracted for clarity.

value over a very large region. However, this shielding is, for the values of the applied field considered here, basically produced by the strips in the two outer vertical columns, which are largely penetrated by currents. Only a little current is needed to flow in the upper and bottom strips of the inner column to create a fine adjustment of the field in the central region.

2. Isolated strips

We now present the results calculated for the case that the superconducting strips are isolated so that current has to go and return always through the same filament. We start again with the case of an x array composed of three strips with dimensions $b/a = 0.1$. In Fig. 7 we show the current profiles and the field distribution calculated for three x arrays with varying separation between the individual strips. The applied field is $0.1 H_{pen}$. Again, all strips have dimensions $b/a = 0.1$. By simple inspection, one can realize how important the differences are with respect to the case of interconnected strips. In the present case of isolated strips there is appreciable current penetration in all strips and not only in outer ones, although the magnetic coupling between them makes the current distribution in the outer strips different from the central one in the case $d/a = 0.02$. Another important effect to be remarked upon is that there is an important flux compression in the space between the strips. Since all strips tend to shield the magnetic field in their interiors independently, the field in the air gap between each pair of strips is stronger because of the field exclusion in both adjacent strips. Actually, field lines are very dense not only in the gap between strips but also in a zone in the strips nearest to the gap, where the current penetrates an important distance (this effect is particularly clear for the case of the smallest separation). This compression effect was also found by Mawatari for the case of x arrays of very thin strips,[31] by Fabbricatore and co-workers for x arrays, xz matrices, and realistic shapes of multifilamentary tapes in the Meissner state,[30,54] and by Mikitik and Brandt for a completely shielded double strip.[55]

We can better compare the current and field profiles for the interconnected and isolated cases by looking at Fig. 8, where we plot current profiles for the x array with separation $d = 0.2a$ for both interconnected and isolated cases. It can be seen that for interconnected strips, current penetrates earlier (that is, for lower values of the applied field) in the outer strips, since current flowing there creates an important shielding not only in each strip but in the whole space between them. On the other hand, in the isolated strips case current returning through the same strip creates a field compression in the channels (which include the gaps and a portion of each strip near the gap), so that the amount of current penetration is similar for the three strips. The current distribution when the strips are close to each other is slightly asymmetric with respect to the central plane of each strip, because the field in the channels felt by the inner sides of the outer strips has a different spatial distribution than the homo-
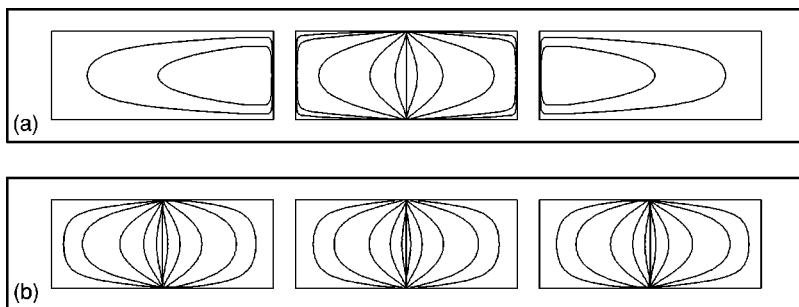

FIG. 8. Current profiles for x arrays with $b/a = 0.1$ and $d/a = 0.2$ for (a) interconnected strips and (b) isolated strips. The vertical axis has been expanded for clarity. The applied field values corresponding to each current profile are $H_a = 0.1$, 0.2, 0.4, 0.6, 0.8, and 1 in units of the penetration field H_{pen} for each case.
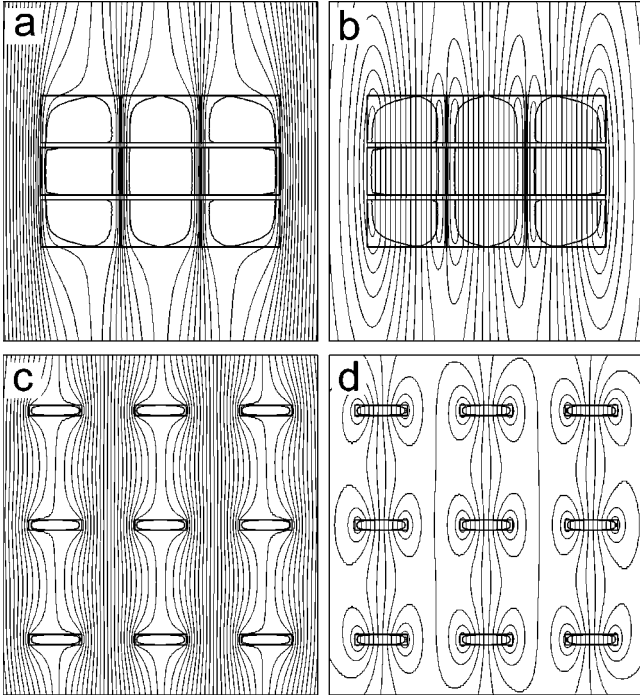
FIG. 9. Total (left) and self (right) magnetic field lines and current profiles for isolated xz matrices at an applied field $H_a = 0.1 H_{pen}$. For the strips $b/a = 0.1$ and $d/a = h/a = 0.02$ (a),(b), and 2 (c),(d).

geneous applied field felt in the outer sides. We have found that this asymmetry increases for thicker filaments, that is, higher b/a (not shown).

We now present some results for the xz-matrix array for the case of isolated strips. As said above, results for the matrix can be understood from the composition of the effects of horizontal and vertical arrays. In Fig. 9 we show the calculated current penetration profiles for an xz array made of nine strips (3×3) with dimensions $b/a = 0.1$ corresponding to an applied field of $0.1 H_{pen}$, together with the total (left figures) and self (right) magnetic field. The two cases correspond to separations of $d/a = h/a = 0.02$ and 2, respectively. The effect of flux compression along the vertical channels that include the gaps and the surrounding regions is clearly seen in the case of the smallest separation distance.

For the case of xz matrices it can be observed how field is shielded in the vertical gaps between rows but it is enhanced in the horizontal gaps between columns. Then, for isolated strips, the magnetic interactions between rows and columns have opposite effects. Furthermore, the difference between the field in the vertical gaps and the applied field H_a is much higher than for the horizontal gaps, as can be seen in Fig. 9 for the xz matrix with higher separation. This implies that the magnetic coupling between strips in the horizontal direction is lost at smaller distances than that in the vertical direction.

IV. MAGNETIZATION

A. Vertical stacks

In this section we analyze the magnetization of the arrays, calculated from the currents following Eq. (4). The reverse and returning curve can be obtained from the initial one using Eqs. (1) and (2).

There are several important properties of the arrays that can be understood from the magnetization results. In Fig. 10 we plot the calculated magnetization M as function of the applied field H_a for a set of three arrays, each with semiside ratio b/a of 0.01 and with different separations $h/a = 0.02$, 0.2, and 2, respectively. We also plot the magnetization for a single strip with $b/a = 0.01$ and another one with $b/a = 0.03$ corresponding to the case that the three strips are one on top of each other. One can observe that the general trend is that the saturation magnetization remains the same for all cases, whereas the initial slope of the magnetization curve changes. The slope is largest in absolute value for the case of a single thin strip ($b/a = 0.01$), has intermediate values for the three arrays (the largest slope is for the array with large separation and smallest for the one with the smallest one),
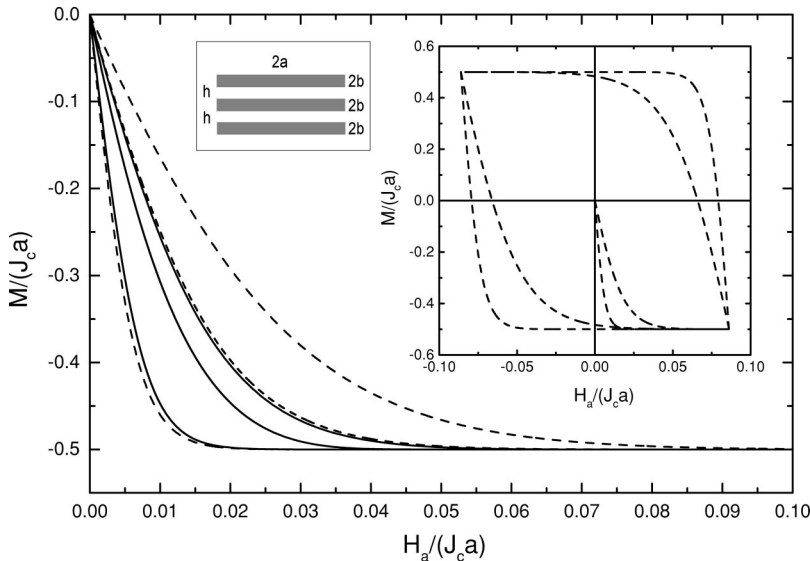

FIG. 10. Initial magnetization as a function of the applied field for, from left to right: a single strip with $b/a = 0.01$, a vertical array of three strips with $b/a = 0.01$ separated a distance $h/a = 2$, the same array with a separation distance of $h/a = 0.2$, the same array with a separation distance of $h/a = 0.02$, a single strip with $b/a = 0.03$, and a single strip with $b/a = 0.05$. In the inset complete magnetization loops are plotted for the first and last cases.
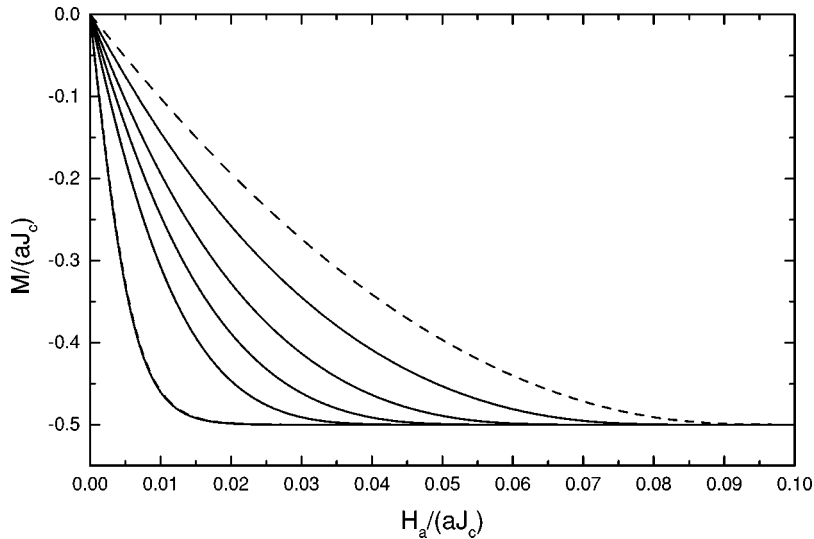
FIG. 11. Initial magnetization as a function of the applied field for, from left to right: a single strip with $b/a=0.01$, the theoretical expression for thin strips (almost overlapped), a set of three strips arranged vertically with $b/a=0.01$ each, a set of 5 strips with $b/a=0.01$ each, a set of 9 strips with $b/a=0.01$ each, a set of 25 strips with $b/a=0.01$ each, and the expression given by Mawatari (Ref. 30) for an array of infinite number of strips of dimensions $b/a=0.01$. The separation distance between the strips in all cases is $h/a=0.2$.

and finally the case with $b/a=0.03$, which, interestingly, is hardly distinguishable from the array with the smallest separation. The reason for such an enhancement of the initial slope is the demagnetizing effect associated with the large sample aspect ratio, according to which the thinner the sample, the larger the initial slope.[27,24] In the arrays for which the separation between the strips is small, the magnetic coupling increases, in agreement with the discussion in Sec. III, so that the sample is behaving as having a larger thickness and, therefore, less demagnetizing effects and less initial slope. In order to study in more detail this effect, we have included in Fig. 10 the calculated magnetization of a single strip with $b/a=0.05$; this strip corresponds to the array with $h/a=0.02$ but as if the gaps between the strips were filled by superconducting material as well. We can see that this case has the smallest slope, and there are large differences with respect to the case of the array of three strips with separation $h/a=0.02$. From these results we can conclude that, provided that the strips are close enough, the behavior of a z stack is similar to that of a single strip with a thickness equal to the sum of the thickness of the superconducting

regions of the z stack, and not the total thickness of the z stack including the gaps.

Another interesting feature to study is the effect of the addition of more strips to the array. We compare in Fig. 11 the calculated $M(H_a)$ curves for arrays with a fixed distance ($h=0.2$) and a different number of strips. We include in the figure the two analytically known limits of one infinitely thin strip[18] and for an infinite set of strips.[31] Results show a practical coincidence between the calculated results for a single strip with finite although small thickness and the results from the analytical formula for very thin strips.[18] With adding more strips, the initial slope of the magnetization (defined as the magnetic moment divided by volume, so independent of the superconductor volume) gets smaller in absolute value. We find that even the case of 25 strips is significantly different from the Mawatari case for an infinite stack, so we can conclude that Mawatari's formula should be valid only for a very large number of strips. In Fig. 12 we show the magnetization curves $M(H_a)$ for arrays of strips separated a larger distance ($h/a=2$). It can be observed that now the differences in the slope are smaller than in the previous case, because there is less magnetic coupling among the strips.
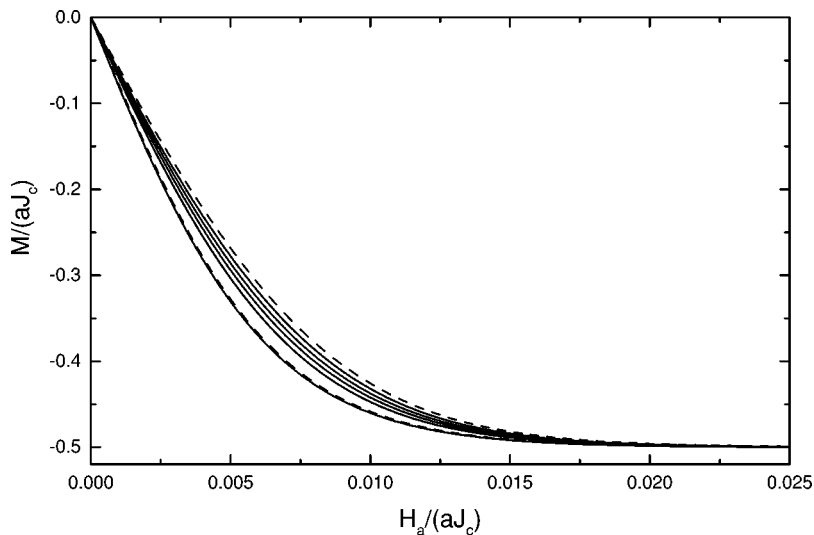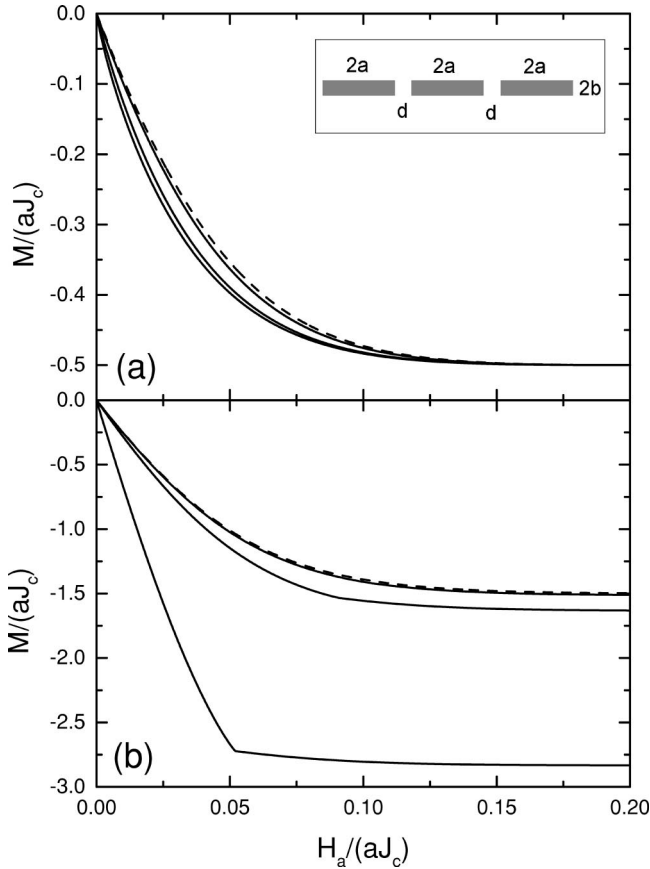

FIG. 12. Same as Fig. 11, but for a separation $h/a=2$.

FIG. 13. Initial magnetization curves $M(H_a)$ for x arrays with three strips with $b/a = 0.1$ and several strip separations d/a for the cases of (a) isolated strips and (b) interconnected strips. For graph (a) solid lines correspond to x arrays with $d/a = 2$, 0.2, and 0.02 from top to bottom, while the dashed line represents $M(H_a)$ for a single strip with $b/a = 0.1$. For graph (b) solid lines correspond to x arrays with $d/a = 0.02$, 0.2, and 2 from top to bottom and the dashed line is for a single strip with half-width $a' = 3a$ and $b = 0.1$.

B. Horizontal arrays

We now analyze the results for the magnetization of the x arrays. In Fig. 13 we plot the calculated magnetization M as function of the applied field H_a for the three x arrays of Figs. 5 and 7. For each strip $b/a = 0.1$, and the separation distance between strips is $d/a = 0.02$, 0.2 and 2. The upper figure shows the results for the isolated strips whereas the data in the bottom part are for interconnected strips.

The magnetization for both isolated and interconnected strips shows important differences, arising from the different current penetration profiles studied in Sec. III. We first discuss the results for isolated strips. It can be seen that M saturates at smaller values than for the case of interconnected strips and that this saturation value is the same for the different separations. The results for the largest separation, $d/a = 2$, are not very different from the results obtained from a single strip with $b/a = 0.1$, corresponding to the limit of complete magnetically uncoupled strips, which is also shown in the figure. An important result is that the initial slope of the $M(H_a)$ curve χ_0 increases (in absolute value) with de-

creasing separation. The reason for this behavior can be traced back to the presence of the flux compression effect discussed in Sec. III B, since a smaller separation means thinner channels and a corresponding larger flux compression. The enhancement of the initial slope can also be explained by the fact that the strips have to shield not only the external applied field but also the field created by the other strips. This enhancement of χ_0 has already been predicted in other related situations.[31,30,54,37]

We have found that the initial slope calculated with our approach is coincident, within a 4% difference, with that calculated numerically by finite elements by Fabbricatore et $al.$[30] for the case of 5×5 and 5×3 filament matrices with complete shielding. The initial slope has also been compared with other works[56,57] for a single strip for a high range of b/a ($0.001 \leqslant b/a \leqslant 100$), obtaining a difference smaller than a 1%.

When comparing the results for isolated strip to the case of interconnected ones, important differences appear. The first difference is that the saturation magnetization in the latter case is not only larger in general with respect to the isolated case but also depends on the separation. The second difference is that the trend found when decreasing the separation distance between strips is reversed: whereas for isolated strip decreasing separation distance d/a results in a larger (in absolute value) slope of the initial magnetization, for interconnected strips the slope gets smaller with decreasing separation.

We explain the reasons for both differences as follows. The different behavior in the saturation magnetization arises from the fact that this value corresponds to the magnetic moment per unit volume when all the strips are fully penetrated. The magnetic moment is proportional to the area threaded by the current loops, which in the interconnected case are not restricted to a single strip but they can span from even one extreme of the array to the other. Actually, the saturation magnetization M_s can be analytically calculated considering that, for isolated strips, at saturation the $\pm J_c$ interface is close to a straight line, so that M_s is the same as for a single uncoupled strip, being $M_s = (1/2)J_c a$.[14,17] For the case of interconnected strips, the current distribution at saturation is $\mathbf{J} = -J_c \hat{\mathbf{y}}$ for $x \geqslant 0$ and $\mathbf{J} = J_c \hat{\mathbf{y}}$ for $x \leqslant 0$, so that M_s can be calculated as

$$M_s = \frac{J_c a}{2}\left[1 + \frac{d}{2a}\right]n_{f,x} \quad (n_{f,x} \text{ even}), \tag{7}$$

$$M_s = \frac{J_c a}{2}\left[n_{f,x} + \frac{d}{2a}\left(n_{f,x} - \frac{1}{n_{f,x}}\right)\right] \quad (n_{f,x} \text{ odd}), \tag{8}$$

where $n_{f,x}$ is the number of strips in the x direction for either an x array or an xz matrix.

As to the initial slope of the $M(H_a)$ curve, in the case of interconnected strips the flux compression effect discussed above does not exist, so the reason for the behavior of the initial slope of the $M(H_a)$ curve must be a different one. The governing effects now are the demagnetizing effects arising from the large aspect ratio of the x array taken as a whole. The demagnetizing effects tend to enhance the initial
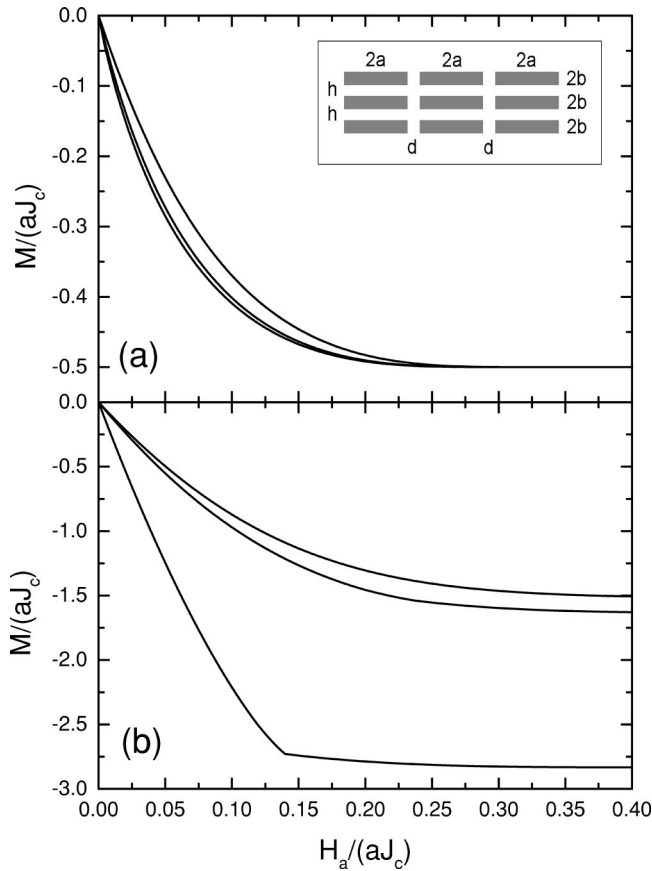
FIG. 14. Initial magnetization curves $M(H_a)$ for xz matrices with 3×3 strips of dimensions $b/a=0.1$, for $h/a=0.2$ and several values of d/a for the cases of (a) isolated strips and (b) interconnected strips. For graph (a) curves correspond to $d/a=2$, 0.2, and 0.02 from top to bottom. For graph (b) curves correspond to $d/a=0.02$, 0.2, and 2 from top to bottom.

slope[27,58,45] when the sample aspect ratio increases. Therefore, when the separation is small the array is behaving similarly to a single strip with the same thickness but 3 times the width, which shows less demagnetizing effect and, as a re-

sult, a smaller (in absolute value) initial slope of the magnetization.

Another feature observed in the interconnected case is the observation of a kink (change in the slope) in the magnetization curve, particularly for the cases of a large separation between strips. This effect is explained as follows. Since the magnetic moment is proportional to the area enclosed by the loops, currents in the external strips contribute more to the magnetization than those in the inner ones. So, when the external strips become saturated, new current can only be induced in the central strip, having a lower contribution to the magnetization M, so that the M rate when H_a is increased is lower in magnitude; a similar effect has been predicted for rings in the critical-state model.[52] In a single strip or even in the case of an x array with isolated filaments, this process is continuous, but not in the present case of interconnected strips separated a horizontal distance.

C. Matrix arrays

The magnetization of xy matrices is again a combination of the effects discussed above for horizontal and vertical arrays. In Fig. 14 the initial magnetization curve $M(H_a)$ for xz matrices with the same vertical separation is plotted, for a vertical separation $h/a=0.2$, and several horizontal separations d/a. The curves are qualitatively similar to those for x arrays and the same values of d/a, so that the discussion done for x arrays is still valid. The main difference between x arrays and xz matrices lies in both the value of the saturation field H_s, that is, the field which M reaches its saturation value, and the magnitude of the initial slope. For the case of both isolated and interconnected xz matrices, H_s is higher than for x arrays, while the initial slope is lower. This is due to the reduction of the demagnetizing effects owing to the stacking in the z direction.[31,30] Moreover, the differences mentioned of the $M(H_a)$ curve between x arrays and matrices would be qualitatively the same if we considered an x array with a larger filament thickness. Detailed results of the magnetization of xz matrices calculated by our model will be presented elsewhere.
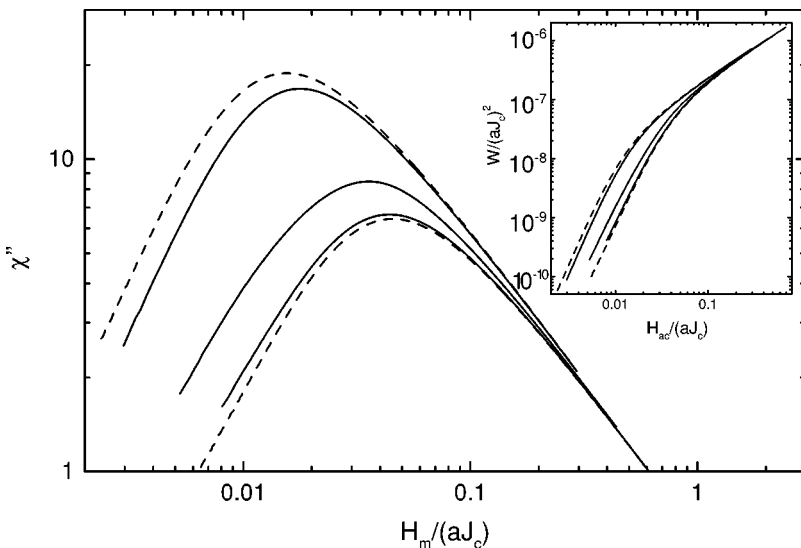

FIG. 15. Imaginary part of the ac susceptibility, χ'', as a function of the amplitude of the ac field H_m corresponding to the curves of Fig. 10, in the same order (the case of a single strip with $b/a=0.05$ is not plotted in this figure). The corresponding power losses are shown in the inset.
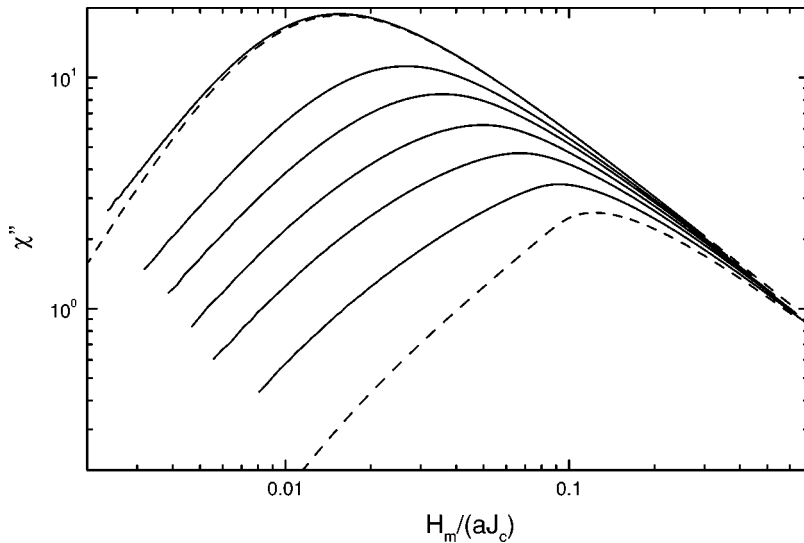
FIG. 16. Imaginary part of the ac susceptibility, χ'', as a function of the amplitude of the ac field H_m corresponding to the curves of Fig. 11, in the same order.

V. ac LOSSES

A. Vertical stacks

In this section we study the imaginary part of the ac susceptibility, χ'', calculated from the magnetization loops from Eq. (5). Here χ'' is directly related to the power losses by Eq. (6).

We present in Fig. 15 the calculated results for χ'' as function of the maximum applied ac field H_a corresponding to the magnetization curves of Fig. 10. All curves show a peak at some value of the applied field amplitude. It can be seen that the peak corresponding to the maximum in χ'' [and therefore a change in slope of the ac losses, since they are proportional to χ'' times H_a^2 as seen in Eq. (6)] is shifting to higher fields and decreasing in magnitude with decreasing separation distance. The reason for that can be obtained from the analogous shifting in the initial slope of the magnetization shown in Fig. 10. Since the ac losses are related to the area of the $M(H_a)$ curve [Eqs. (5) and (6)] and the magnetization saturation is the same for all cases, the key factor for the loss behavior is the initial slope governed by the demagnetizing effects as discussed in Sec. IV.

The results in Fig. 15 show that the $\chi''(H_a)$ curve goes as H_a^n for low fields, with n ranging from 1.5 for a strip with $b/a = 0.01$, corresponding to the high h/a limit for a z stack, to 1.3 for a strip with $b/a = 0.03$, being the low-h/a limit for arrays. These values lie between the known limiting values for infinite slabs ($n = 1$) (Ref. 14) and thin strips ($n = 2$). The corresponding power losses [related to χ'' by Eq. (6); see inset] go therefore as H_a^n, with n ranging from 3.5 to 3.3. For high fields, χ'' goes as H_a^{-1} in all cases.

In Figs. 16 and 17 we calculate the results for χ'' as function of the maximum applied ac field H_a with the goal of studying the effect of adding more strips in the array. We use the same cases as in Figs. 11 and 12, corresponding to two different separations in the arrays ($h/a = 0.2$, and 2, respectively). Again, there is a close relation between the increase in the initial slope of the magnetization curves and the shifting of the position of the peak in χ'' to higher fields. It is interesting to comment, however, that the formulas provided by Mawatari for the case of an infinite array are not adequate to describe quantitatively the ac losses of a finite array even if the array consists of up to 25 strips.
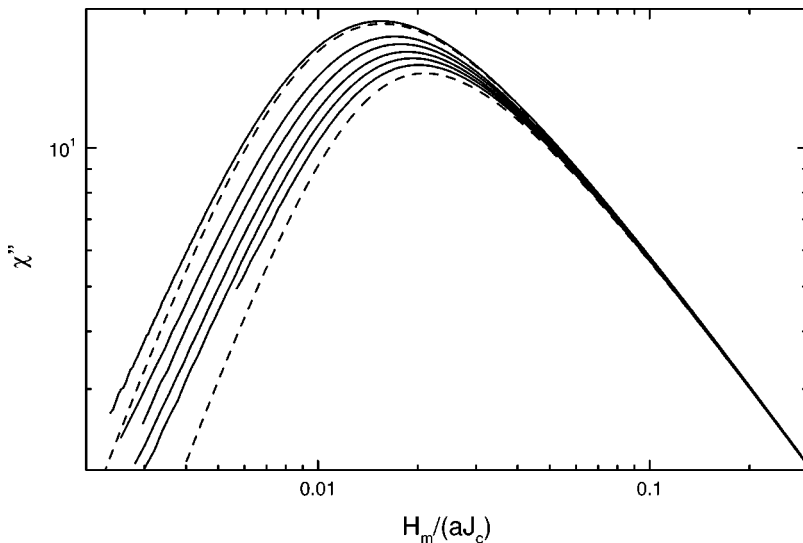

FIG. 17. Imaginary part of the ac susceptibility, χ'', as a function of the amplitude of the ac field H_m corresponding to the curves of Fig. 12, in the same order.
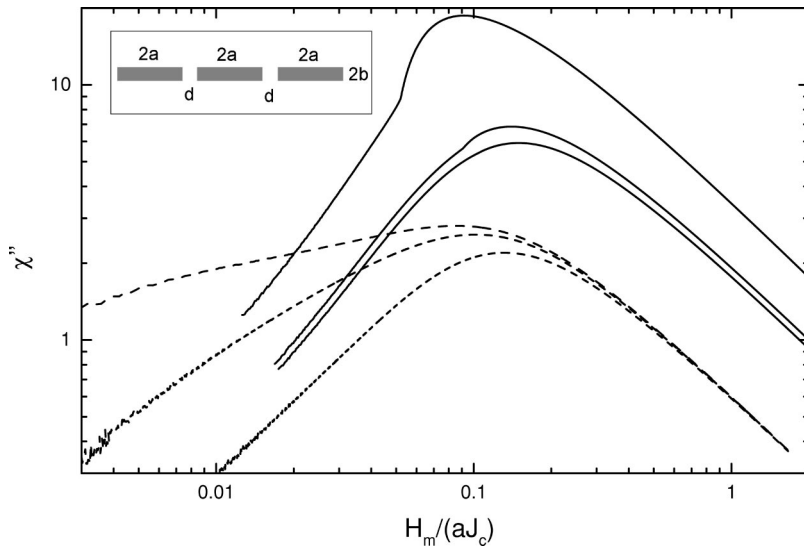
FIG. 18. Imaginary ac susceptibility χ'' as a function of the ac applied field amplitude H_{ac} corresponding to the $M(H_a)$ curves showed in Fig. 13 for x arrays. The strips dimensions are $b/a = 0.1$. Solid lines are for the case of interconnected strips for $d/a = 2$, 0.2, and 0.02 from top to bottom, while dashed lines are for isolated strips with $d/a = 0.02$, 0.2, and 2 from top to bottom.

It is clear from the calculations presented in this section that in order to reduce the magnetic contribution to the ac losses in a real superconducting tape with a z-stack geometry one should increase the coupling of the filaments by decreasing the distance between them (see Fig. 15). Also, the results in Fig. 16 and 17 show that the ac losses decrease with increasing the number of filaments while keeping the distance between them, particularly in the case of a small separation ($h/a = 0.2$, Fig. 16). These results can be understood again as arising from the effect of demagnetizing fields. When the superconducting strips are separated a small distance, the whole array is acting basically as a single superconducting tape with a thickness equal to the sum of the thickness of the strips, so the demagnetizing effects are less, the initial magnetization has a smaller slope (in absolute value) as discussed in Sec. V, and the area of the hysteresis loops is less for a given maximum applied ac field, so that the ac losses are reduced. On the other hand, when the separation of the strips gets larger, the magnetic coupling between them is less so that they act more like magnetically decoupled filaments with high aspect ratio and the demagnetizing effects act more, increasing the ac losses. It is interesting to notice that when we talk about the separation h being small one should understand it as small compared with the horizontal dimension $2a$ and not to the strip thickness $2b$. Calculations of the same values of h/a for the case $b/a = 0.1$ (instead of $b/a = 0.01$ as in the results presented above), for example, yield qualitatively the same effects for the same h/a values.

B. Horizontal arrays

In this section we study the imaginary part of the ac susceptibility, χ'', calculated from the magnetization loops obtained in Sec. IV, which can be easily related to the ac losses.[59] In Fig. 18 we present calculated results for χ'' as function of the ac field amplitude H_{ac} for the same x arrays discussed in the previous sections (with $b/a = 0.1$ and different separation distances $d/a = 2$, 0.2, and 0.02). The two different cases of interconnected and isolated strips are plotted together for comparison. The results show that the general trend is the appearance of a peak in the χ'' curve (and therefore a change of slope of the ac losses). This peak, however, is wider for the case of isolated strips (also shown in the figure), especially on the left part of the peak. This effect has been experimentally found in several works.[28,29,60,61] Actually, the cause of the disagreement between theoretical predictions and experiments in these works is that they used models for single strips or disks, which yielded narrow peaks. Our model allows for the explanation of this effect. Concerning hysteresis losses only, as we do in this work, the reason for this widening of the peak is that the $M(H_a)$ curve becomes nonlinear at small applied field values because of the penetration of magnetic flux not only in the outer surface regions of the strips but also in the channels between strips, where the field intensity is enhanced. This deviation from linearity in the $M(H_a)$ curve results in an increase of the loss.

We also find that decreasing the distance between strips results in a higher or a smaller value of the peak, depending upon whether we are considering the isolated or interconnected case, respectively. This dependence on the separation distance is only slight for the case of isolated strips and much more evident for the interconnected ones. These results can be understood from the magnetization curves of Fig. 13, in which we observe two important properties: the initial slope of the magnetization curve for interconnected strips increases (in absolute value) with increasing distance between strips, while it decreases for isolated strips, and, most important, for interconnected strips, the saturation magnetization has very different values for the different separations, while it remains almost constant for isolated strips. All these effects have been explained in Sec. IV. Another characteristic observed in the two upper curves of Fig. 18 is a kink at a particular field value that is directly related to the presence of a similar kink in the magnetization data shown in Fig. 13. This kink was already predicted for rings[52] and later experimentally observed.[62] Furthermore, experimental evidence of a kink in actual superconducting tapes was shown for the case of a
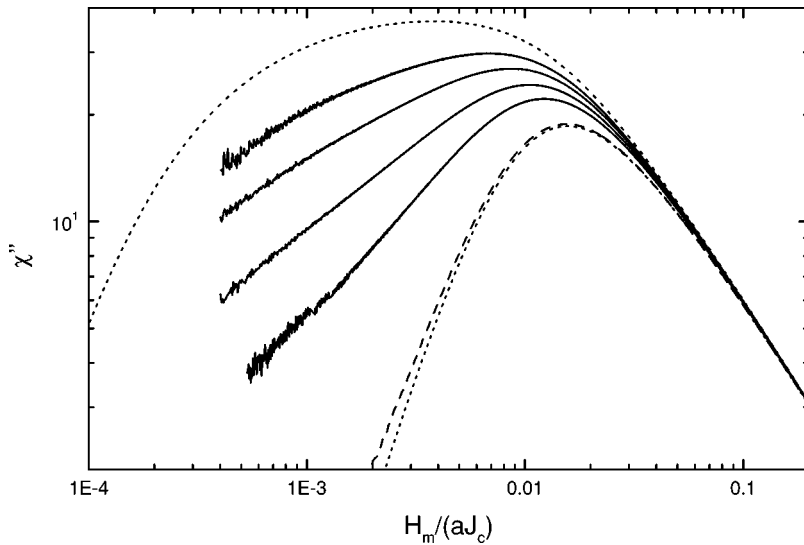
FIG. 19. Imaginary ac susceptibility χ'' as a function of H_{ac} for x arrays with several numbers of strips n_f (solid lines), corresponding to $n_f = 9, 5, 3, 2$ from top to bottom, compared to a single strip (dashed line) and the analytical limits for a single thin strip (lower dotted line) and an infinite x array of thin strips (upper dotted line). The strips dimensions are $b/a = 0.01$.

Ag/Bi-2223 tape with the superconducting core shaped as a circular shell[63] or two concentric elliptical shells.[40]

Another interesting result for the χ'' calculations is shown in Fig. 19, where we show the calculated results for x arrays of several strips with $b/a = 0.01$ with a fixed separation distance of $d/a = 0.02$. Results are shown for arrays of two, three, five, and nine strips. We consider the isolated strips case, in order to compare our results with the analytical prediction for an infinite array of Mawatari.[31] We also include the calculated result for a single strip with $b/a = 0.01$ as well as the same curve calculated from the analytical formulas for thin strips.[18] On the other limit, we check that the results for a large number of strips tend to the analytical results of Mawatari,[31] although 9 is not a sufficient number for approaching the limiting case (higher number of strips yield values closer to Mawatari's results; not shown for clarity). The general trend observed is that the losses increase with the number of strips is due to the fact that the effect of the channels discussed above increases for higher number of strips.[30,54,37]

C. Matrix arrays

In Fig. 20 we present the dependence of χ'' upon the ac applied field amplitude H_{ac} for xz matrices with $b/a = 0.1$, $h/a = 0.2$, and several values of d/a. It can be seen that the qualitative variations of the $\chi''(H_{ac})$ curve when considering isolated or interconnected strips is the same as for x arrays, as well as the effect of changing d/a. However, for xz matrices there is both a reduction of the peak in the $\chi''(H_{ac})$ curve and a shifting to higher H_{ac} values. These facts can be explained returning to the initial magnetization curves in Figs. 13 and 14, where the initial slope was lower for all xz matrices and the saturation field was higher. A detailed study of the ac losses from the χ'' values, including the real part of the susceptibility, χ', for xz matrices will be presented elsewhere.

VI. CONCLUSIONS

We have presented a numerical model for calculating current penetration profiles and field lines and magnetization
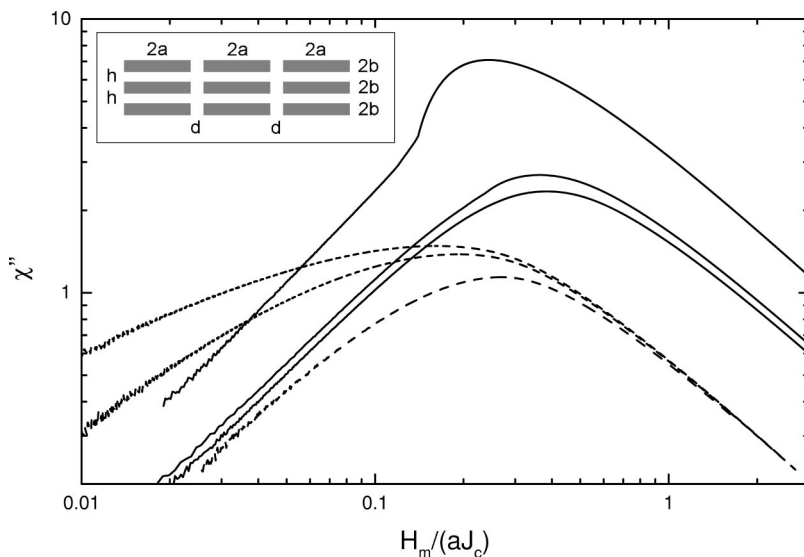

FIG. 20. Imaginary ac susceptibility χ'' as a function of H_{ac} corresponding to the $M(H_a)$ curves showed in Fig. 14 for xz matrices. The strips dimensions are $b/a = 0.1$ and the vertical separation is fixed, being $h/a = 0.2$. Solid lines are for the case of interconnected strips for $d/a = 2, 0.2,$ and 0.02 from top to bottom, while dashed lines are for isolated strips with $d/a = 0.02, 0.2,$ and 2 from top to bottom.

and ac losses of arrays of superconducting strips. In this work we have analyzed the cases of arrays arranged in vertical, horizontal, and matrix configurations. We have found that the demagnetizing effects have strong influences on both the magnetic response of the tapes and the ac losses appearing when an ac magnetic field is applied.

For vertical stacks of strips, we find that the intial magnetization (in absolute value) and the ac losses are reduced when decreasing the vertical separation between filaments. When the vertical separation is small as compared with the filaments width, then the array is behaving as a single filament with thickness the sum of the superconducting material. These results could be used as guides for designing actual superconducting tapes. Then, in order to optimize the losses, for filaments with a fixed aspect ratio, it is preferable to have a large number of them separated small distances so that there is a good magnetic coupling between them, as has been already experimentally found.[28]

For horizontal and matrix arrays, the different cases of isolated and completely interconnected strips have been discussed separately. Current penetration results show that whereas in the interconnected cases the filaments magnetically shield the whole internal volume of the array, in the case of isolated strips, the shielding is within each of them. The latter effect in the isolated strip case creates channels of field compression between the strips, particularly when the separation distance between them is small. These channels govern the magnetic and ac losses properties of the arrays of isolated strips. Because of them, when decreasing the horizontal distance between strips, the initial slope of the magnetization curve increases (in absolute value), and, correspondingly, there are larger ac losses. Moreover, the experimentally found effect of a widening of the peak in the imaginary part of the ac susceptibility can be explained by the same effect. On the other hand, for the case of interconnected strips, the trend is the opposite: decreasing the horizontal distance between strips reduces both the initial slope of the magnetization curve and the ac losses. The effects governing these latter features are now the demagnetizing effects: when strips are close to each other they behave as a single strip with smaller aspect ratio and, therefore, with smaller demagnetizing effects.

The magnetic properties of superconductor matrix arrays are a composition of those for horizontal and vertical arrays. A result of practical importance is that ac losses are reduced when decreasing the vertical separation between strips in the tape, because when stacking strips in the vertical direction they behave as thicker strips and therefore have less demagnetizing effects and less ac losses.

In the present version, the model cannot be used to the study of the case in which a transport current flows in the array in addition to those induced by the applied magnetic field. This extension will be presented elsewhere.

APPENDIX A: FIELD OF FULL PENETRATION

In this appendix we present a simple way to analytically calculate the field of full penetration of the array, H_{pen}, defined as the minimum applied field in the initial magnetization curve for which current fills the whole of the superconducting region. The penetration field can be calculated in general as minus the field generated by the current distribution $\mathbf{H}_J$ in the last induced current point, where $\mathbf{H}_J = H_J \hat{\mathbf{z}}$.[24,64] So both the current distribution at the penetration field and the last induced current point position $\mathbf{r}_m$ must be known to calculate H_{pen}.

1. Vertical arrays

In the geometry of a set of rectangular cross-section strips ordered as a z stack we can distinguish two different cases, depending on whether the number of strips n_f is odd or even. Although in both cases the current distribution at H_{pen} is evident, it is not so for $\mathbf{r}_m$. The last induced current point can be found as where the field generated by the currents is maximum in magnitude, since $\mathbf{r}_m$ is the last point where external field is shielded. For the odd number of strips case, $\mathbf{r}_m$ is simply the position of the center of the central strip, although it is not so easy to determine when the number of strips is even.

For a z stack of an odd number of strips n_f with dimensions $2a$ and $2b$ in the x and z directions separated a distance h the penetration field is therefore

$$H_{\text{pen}}(a,b,h,n_f)$$

$$= \frac{J_c}{2\pi}\left[F_1(0,a,b) + 2 \sum_{i=1}^{(n_f-1)/2} F_1((2b+h)i,a,b) \right]$$

$$(n_f \text{ odd}), \tag{A1}$$

where $F_1(u,t,d)$ is defined as

$$F_1(u,t,d) = 2t\left\{ \arctan\frac{u+d}{t} - \arctan\frac{u-d}{t} \right\}$$

$$+ (u-d)\ln\left[\frac{(u-d)^2}{t^2+(u-d)^2} \right]$$

$$+ (u+d)\ln\left[\frac{(u+d)^2}{t^2+(u+d)^2} \right]. \tag{A2}$$

Equation (A1) has been derived using the expression for the magnetic field created by a completely penetrated strip with uniform J_c calculated by direct integration of the Biot-Savart law. The case $n_f=1$ reproduces the known result for the penetration field for a strip.[24]

As mentioned above, when a z stack has an even number of strips we must find the last point where current is induced, at which the self-field H_J is maximum in magnitude. Owing to the symmetry of the current fronts in the yz plane, this point will be on the z axis. Thus, only maximization of $H_{J,z}$

along the z axis is needed. Since the maximization of the field $H_{J,z}$ is different for every specific value of n_f, we only report the result for $n_f=2$, which is the most important case, concerning the magnetic coupling, for an even n_f. Then, the last induced current point will be at a position

$$
z_m^2 = \frac{1}{2}[-a^2 - h\beta
$$
$$
+ \sqrt{(a^2+h\beta)^2 + h\beta(2a^2+h^2/2+2\beta^2+h\beta)}],
$$

$$(A3)$$

z_m being the z component of $\mathbf{r}_m$ and β defined as $\beta=2b+h/2$. The penetration field for two strips is

$$
H_{\text{pen}}(a,b,n_f=2) = \frac{J_c}{2\pi}[F_1(z_m-b-h/2,a,b)
$$
$$
+ F_1(z_m+b+h/2,a,b)], \quad (A4)
$$

where the function $F_1(u,t,d)$ is defined in Eq. (A2).

2. Horizontal and matrix arrays

For x arrays and xz matrices we differentiate again two cases depending on the way that the strips are connected at infinity: completely interconnected strips and current isolated strips.

a. Completely interconnected strips

For this case, the volume current density at the penetration field is $\mathbf{J}=-J_c\hat{\mathbf{y}}$ for $x>0$ and $\mathbf{J}=J_c\hat{\mathbf{y}}$ for $x<0$.

When both the number of strips in the x axis $n_{f,x}$ and in the z axis $n_{f,z}$ are odd, the last induced current point $\mathbf{r}_m$ is simply the center of the central strip. Using the Biot-Savart law to calculate $H_{J,z}(\mathbf{r}=0)$, we obtain

$$
H_{\text{pen,matrix}}(n_{f,x},n_{f,z})
$$

$$
= H_{\text{pen,stack}}(n_{f,z}) + \frac{J_c}{2\pi}\left[2\sum_{i=1}^{(n_{f,x}-1)/2} F_2((2a+d)i,0,a,b)\right.
$$

$$
\left. + 4\sum_{i=1}^{(n_{f,x}-1)/2}\sum_{j=1}^{(n_{f,z}-1)/2} F_2((2a+d)i,(2b+h)j,a,b)\right],
$$

$$(A5)$$

where $H_{\text{pen,stack}}$ is the penetration field for a z stack and the function $F_2(u,v,t,d)$ is defined as

$$
F_2(u,v,t,d) = (u-t)\left[\arctan\left(\frac{v-d}{u-t}\right) - \arctan\left(\frac{v+d}{u-t}\right)\right]
$$
$$
+ (u+t)\left[\arctan\left(\frac{v+d}{u+t}\right) - \arctan\left(\frac{v-d}{u+t}\right)\right]
$$
$$
+ \frac{(u-d)}{2}\ln\left[\frac{(u-t)^2+(v-d)^2}{(u+t)^2+(v-d)^2}\right]
$$
$$
+ \frac{(u+d)}{2}\ln\left[\frac{(u+t)^2+(v+d)^2}{(u-t)^2+(v+d)^2}\right]. \quad (A6)
$$

The penetration field for an x array with an odd number of strips is the same as in Eq. (A5) but removing the term with the double sum and taking $n_{f,z}=1$.

When either $n_{f,x}$ or $n_{f,z}$ are even, the last induced current point is not easy to be determined. In those strips that current returns through the same filament, the total magnetic field increases monotonically from the edges of the strip to the current profile. When $n_{f,x}$ is odd and $n_{f,z}$ is even the last strips to be fully penetrated are those in the central column and in the inner rows. Then, the last induced current point $\mathbf{r}_m$, where $H_{J,z}(\mathbf{r}_m)=-H_{\text{pen}}$, is on the z axis and can be determined as the point where $H_{J,z}$ is maximum in absolute value. When $n_{f,x}$ is even, we have found no way to analytically calculate $\mathbf{r}_m$ and H_{pen}.

b. Current isolated strips

As discussed in Sec. III B, the current interface at the penetration field is almost a vertical straight line at the center of the strip. We have found that this approximation is reasonable even for strips with a ratio b/a as large as $b/a=1$.

When $n_{f,z}$ is odd, the last penetrated current point is at the center of the strips belonging to the central row and the most external columns. This is so because external rows shield inner ones and external columns increase the field on the inner ones. Then, using the Biot-Savart law and assuming straight current interfaces, the penetration field for an xz matrix with odd $n_{f,z}$ is

$$
H_{\text{pen,matrix}}(n_{f,x},n_{f,z}) = \frac{-J_c}{2\pi}\left[\sum_{i=0}^{n_{f,x}-1} F_3((2a+d)i,0,a,b)\right.
$$

$$
+ 2\sum_{i=0}^{n_{f,x}-1}\sum_{j=1}^{(n_{f,z}-1)/2} F_3
$$

$$
\left. \times((2a+d)i,(2b+h)j,a,b)\right],
$$

$$(A7)$$

where the function $F_3(u,v,t,d)$ is defined as $F_3(u,v,t,d) = F_2(u-t/2,v,t/2,d) - F_2(u+t/2,v,t/2,d)$. Notice that Eq. (A7) is valid when $n_{f,x}$ is either odd or even, while Eq. (A5) is only valid for an odd $n_{f,x}$. The penetration field for an x array is the same as described in Eq. (A7) but removing the term with the double sum.

APPENDIX B: CALCULATION OF INDUCTANCES

In this appendix we calculate the self- and mutual inductances used in Eq. (3). These inductances are calculated for closed circuits of the shape of a pair of identical rectangular infinite prisms of dimensions $2a'\times2b'$ carrying uniform current density. The prisms are set symmetrically to the zy plane, taking the y axis parallel to the infinite direction. The current of the prism set in the $x\geq0$ region is taken positive, while it is taken negative for the other.

The self- and mutual inductances are calculated from the magnetic energy using the equation[48]

$$M_{ij}I_iI_j = W_{ij} = \int_{x_i-a'}^{x_i+a'}dx\int_{z_i-b'}^{z_i+b'}dzA_{y,j}(x,z)J_i$$

$$- \int_{-x_i-a'}^{-x_i+a'}dx\int_{z_i-b'}^{z_i+b'}dzA_{y,j}(x,z)J_i, \quad \text{(B1)}$$

where M_{ij} is the mutual inductance per unit length of two closed circuits labeled as i and j, respectively, I_i and I_j are the current intensity flowing through the circuits, W_{ij} is the magnetic energy per unit length of the circuits, (x_i,z_i) is the central position of the prism in the $x \geq 0$ region of the i circuit, a' and b' are the dimensions of the prisms in the x and z directions, respectively, and $A_{y,j}$ is the y component of the vector potential created by the circuit j taking the gauge $\nabla \cdot \mathbf{A} = 0$.

The vector potential $A_{y,j}$ can be calculated by direct integration, leading to

$$A_{y,j}(x,z) = \frac{\mu_0 J_j}{2\pi}[F(x-x_j,z) - F(x+x_j,z)], \quad \text{(B2)}$$

where the function $F(u,v)$ is defined as

$$F(u,v) = f(a'-u,b'-v) + f(a'-u,b'+v)$$

$$+ f(a'+u,b'-v) + f(a'+u,b'+v), \quad \text{(B3)}$$

defining $f(t,d)$ as

$$f(t,d) = \frac{1}{2}\left[td\ln(t^2+d^2) - 3td + t^2\arctan\frac{d}{t} + t^2\arctan\frac{d}{t}\right]. \quad \text{(B4)}$$

Taking into account that the current density in the prisms is uniform, M_{ij} can be deduced integrating Eq. (B1) using Eqs. (B2)–(B4), which yield

$$M_{ij} = \frac{\mu_0}{16\pi a'^2 b'^2}[G(x_j-x_i,y_j-y_i) - G(-x_j-x_i,y_j-y_i)], \quad \text{(B5)}$$

where the function $G(u,v)$ is defined as

$$G(u,v) = \sum_{k,l,n,m=1}^{2}(-1)^{k+l+n+m}g(R(k,n)a'$$

$$+ u, R(l,m)b'+v), \quad \text{(B6)}$$

defining $R(i,j) = (-1)^i - (-1)^j$, and the function $g(t,d)$ as

$$g(t,d) = \frac{25}{48}t^2d^2 - \frac{dt^3}{6}\arctan\frac{d}{t} - \frac{td^3}{6}\arctan\frac{t}{d}$$

$$+ \frac{1}{48}(t^4+d^4-6t^2d^2)\ln(t^2+d^2). \quad \text{(B7)}$$

[1] D. Larbalestier, A. Gurevich, D. M. Feldmann, and A. Polyanskii, Nature (London) **414**, 368 (2001).

[2] P. Vase, R. Flukiger, M. Leghissa, and B. Glowacki, Supercond. Sci. Technol. **13**, R71 (2000).

[3] G. Ries, M. Leghissa, J. Rieger, J. Wiezorek, and M. Oomen, Physica C **310**, 283 (1998).

[4] M. N. Wilson, *Superconducting Magnets* (Oxford University Press, Oxford, 1983).

[5] W. J. Carr, Jr., *AC Loss and Macroscopic Theory of Superconductors* (Gordon and Breach, New York, 1983).

[6] A. Oota, T. Fukunaga, T. Abe, S. Yuhya, and M. Hiraoka, Appl. Phys. Lett. **66**, 2128 (1995).

[7] U. Welp, D. O. Gunter, G. W. Crabtree, J. S. Luo, V. A. Maroni, W. L. Carter, V. K. Vlasko-Vlasov, and V. I. Nikitenko, Appl. Phys. Lett. **66**, 1270 (1995).

[8] A. E. Pashitski, A. Polyanskii, A. Gurevich, J. A. Parrell, and D. C. Larbalestier, Physica C **246**, 133 (1995).

[9] K.-H. Müller, Physica C **312**, 149 (1999).

[10] Y. Fukumoto, H. J. Wiesmann, M. Garber, M. Suenaga, and P. Haldar, Appl. Phys. Lett. **67**, 3180 (1995).

[11] M. P. Oomen, J. Rieger, and M. Leghissa, Appl. Phys. Lett. **70**, 3038 (1997).

[12] A. Wolfbrandt, N. Magnusson, and S. Hörnfeldt, IEEE Trans. Appl. Supercond. **11**, 4123 (2001).

[13] T. Chiba, Q. Li, S. P. Ashworth, and M. Suenaga, IEEE Trans. Appl. Supercond. **9**, 2143 (1999).

[14] C. P. Bean, Phys. Rev. Lett. **8**, 250 (1962).

[15] Y. B. Kim, C. F. Hempstead, and A. R. Strnad, Phys. Rev. Lett. **9**, 306 (1962).

[16] D.-X. Chen and R. B. Goldfarb, J. Appl. Phys. **66**, 2489 (1989).

[17] E. H. Brandt, M. Indebom, and A. Forkl, Europhys. Lett. **22**, 735 (1993).

[18] E. H. Brandt and M. Indenbom, Phys. Rev. B **48**, 12 893 (1993).

[19] E. Zeldov, J. R. Clem, M. McElfresh, and M. Darwin, Phys. Rev. B **49**, 9802 (1994).

[20] J. McDonald and J. R. Clem, Phys. Rev. B **53**, 8643 (1996).

[21] P. N. Mikheenko and Y. E. Kuzovlev, Physica C **204**, 229 (1993).

[22] J. Zhu, J. Mester, J. Lockhart, and J. Turneaure, Physica C **212**, 216 (1993).

[23] J. R. Clem and A. Sanchez, Phys. Rev. B **50**, 9355 (1994).

[24] E. H. Brandt, Phys. Rev. B **54**, 4246 (1996).

[25] E. H. Brandt, Phys. Rev. B **58**, 6506 (1998).

[26] T. B. Doyle, R. Labusch, and R. A. Doyle, Physica C **290**, 148 (1997).

[27] A. Sanchez and C. Navau, Phys. Rev. B **64**, 214506 (2001).

[28] F. Gömöry, J. Šouc, A. Laudis, P. Kováč, and I. Hušek, Supercond. Sci. Technol. **13**, 1580 (2000).

[29] F. Gömöry, J. Šouc, P. Fabbricatore, S. Farinon, F. Strýček, P. Kováč, and I. Hušek, Physica C **371**, 229 (2002).

[30] P. Fabbricatore, S. Farinon, S. Innoceti, and F. Gömöry, Phys. Rev. B **61**, 6413 (2000).

[31] Y. Mawatari, Phys. Rev. B **54**, 13 215 (1996); IEEE Trans. Appl. Supercond. **7**, 1216 (1997).

[32] Y. Mawatari and J. R. Clem, Phys. Rev. Lett. **86**, 2870 (2001).

[33] R. Tebano, F. Gömöry, E. Seiler, and F. Stryceck, Physica C **372–376**, 998 (2002).

[34] F. Gömöry, L. Gherardi, R. Mele, D. Morin, and G. Crotti, Physica C **279**, 39 (1997).

[35] A. V. Volkozub, J. Everett, G. Perkins, P. Buscemi, A. D. Caplin, M. Dhallé, F. Marti, G. Grasso, Y. B. Huang, and R. Flükiger, IEEE Trans. Appl. Supercond. **9**, 2147 (1999).

[36] A. V. Volkozub, A. D. Caplin, Y. B. Huang, R. Flükiger, G. Grasso, H. Eckelmann, M. Quilitz, and W. Goldacker, Physica C **310**, 159 (1998).

[37] J. Everett, G. Perkins, A. V. Volkozub, A. D. Caplin, M. Dhallé, A. Polcari, F. Marti, Y. B. Huang, and R. Flükiger, Physica C **310**, 202 (1998).

[38] S. P. Ashworth, B. A. Glowacki, M. Ciszek, E. C. L. Chesneau, and P. Haldar, IEEE Trans. Appl. Supercond. **7**, 1662 (1997).

[39] B. A. Glowacki, C. J. van der Beek, and M. Konczykowski, in Inst. Phys. Conf. Ser. No. 167, edited by X. Obradors, F. Sandiumenge, and J. Fontcuberta (Institute of Physics, London, 2000), Vol. 2, p. 779.

[40] F. Gömöry, L. Gherardi, G. Crotti, D. Bettinelli, L. Martini, L. Bigoni, and S. Zannella, Physica C **310**, 168 (1998).

[41] A. V. Bobyl, D. V. Shantsev, T. H. Johansen, M. Baziljevick, Y. M. Galperin, and M. E. Gaevski, Supercond. Sci. Technol. **13**, 183 (2000).

[42] A. Badia, C. Lopez, and J. L. Giordano, Phys. Rev. B **58**, 9440 (1998).

[43] K. V. Bhagwat, S. V. Nair, and P. Chaddah, Physica C **227**, 176 (1994).

[44] P. Chadah, Pramana, J. Phys. **36**, 353 (1991).

[45] F. M. Araujo-Moreira, C. Navau, and A. Sanchez, Phys. Rev. B **61**, 634 (2000).

[46] C. Navau and A. Sanchez, Phys. Rev. B **64**, 214507 (2001).

[47] A. Sanchez and C. Navau, Supercond. Sci. Technol. **14**, 444 (2001).

[48] L. D. Landau, E. M. Lifshitz, and L. P. Pitaevskii, *Electrodynamics of Continuous Media*, 2nd ed. (Pergamon Press, New York, 1984).

[49] L. Prigozhin, J. Comput. Phys. **129**, 190 (1996).

[50] F. Gömöry, R. Tebano, A. Sanchez, E. Pardo, C. Navau, I. Husek, F. Strycek, and P. Kovac, Supercond. Sci. Technol. **15**, 1311 (2002).

[51] D. Karmakar and K. V. Bhagwat, Phys. Rev. B **65**, 024518 (2001).

[52] E. H. Brandt, Phys. Rev. B **55**, 14 513 (1997).

[53] V. Ivaska, V. Jonkus, and V. Palenskis, Physica C **319**, 79 (1999).

[54] S. Farinon, P. Fabbricatore, F. Gömöry, and E. Seiler, IEEE Trans. Appl. Supercond. **11**, 2776 (2001).

[55] G. P. Mikitik and E. H. Brandt, Phys. Rev. B **64**, 092502 (2001).

[56] E. H. Brandt and G. P. Mikitik, Phys. Rev. Lett. **85**, 4164 (2000).

[57] D.-X. Chen, C. Prados, E. Pardo, A. Sanchez, and A. Hernando, J. Appl. Phys. **91**, 5254 (2002).

[58] E. Pardo, A. Sanchez, and D.-X. Chen, J. Appl. Phys. **91**, 5260 (2002).

[59] D.-X. Chen and A. Sanchez, J. Appl. Phys. **70**, 5463 (1991).

[60] M. Suenaga, T. Chiba, S. P. Ashworth, D. O. Welch, and T. G. Holesinger, J. Appl. Phys. **88**, 2709 (2000).

[61] M. P. Oomen, J. J. Rabbers, B. ten Haken, J. Rieger, and M. Leghissa, Physica C **361**, 144 (2001).

[62] Th. Herzog, H. A. Radovan, P. Ziemann, and E. H. Brandt, Phys. Rev. B **56**, 2871 (1997).

[63] T. Fukunaga, T. Abe, A. Oota, S. Yuhya, and M. Hiraoka, Appl. Phys. Lett. **66**, 2128 (1995).

[64] A. Forkl, Phys. Scr. **T49**, 148 (1993).